Electronic Supplementary Material (ESI) for Journal of Materials Chemistry C.

Supplementary Information

Materials:

All chemical reagents materials were used as received and used without purification, unless otherwise noted. Fluorine-doped tin oxide (FTO) was gotten in Advanced Election Technology Co., Ltd. 99.9% Cesium carbonate (Cs_2CO_3), 99.999% Zinc bromide ($ZnBr_2$), 99.5% Copper bromide ($CuBr_2$), 90% Oleic acid (OA), 95% Hexane and 99.5% Ethyl acetate, which were obtained from Sigma-Aldrich. 99.5% Toluene was from Sinopharm Chemical Reagent Co., Ltd. 99.999% Lead (II) bromide ($PbBr_2$), Oleylamine (OAm, approximate C18 content 80-90%), 99.8% Dimethylsulfoxide (DMSO), 99.9% N, N-dimethylformamide (DMF) were gotten in Advanced Election Technology Co., Ltd. 48 % Hydrogen bromide (HBr) was gotten in Aladdin. 99% Nickel bromide ($NiBr_2$) was purchased from Acros. 99% Iodide lithium (LiI), and 98% Lithium chloride (LiCl) were Acme and Shao Yuan, respectively.

Synthesis of transition metal(II)-doped $CsPb_2Br_5/CsPbBr_3$ perovskite nanocrystals (NCs):

Firstly, OA (2mL) and Cs_2CO_3 (0.2g) reagents were mixed in a 3-neck flask, which were dissolved at 120 °C to formating the Cs-oleate. Synthesis of $CsPb_2Br_5/CsPbBr_3$ perovskite NCs are synthesized in the following two steps: One, the precursor solution was synthesized by V_{OA}/V_{OAm}=2:1 (volume ratio) with 0.24 mmol $PbBr_2$ dissolved in V_{DMF}/V_{HBr}=800:1 (volume ratio). Two, by injecting 2 mL of precursor with 0.05 mL Cs-oleate into 20 mL hexane under vigorous stirring. In addition, the $PbBr_2/MBr_2$ (M=Ni^{2+}, Cu^{2+} and Zn^{2+} reagents) is changed by molar ratio in the precursor to prepare transition metal(II)-doped samples NCs.

Purification of the transition metal(II)-doped $CsPb_2Br_5/CsPbBr_3$ perovskite NCs:

The above NCs solution was centrifuged with 15 % ethyl acetate (10 mL) at 8000 rpm for 5 min. Then, the precipitate was re-dispersed in 6 mL hexane at 5000 rpm for 5 min. Subsequently, the precipitate was re-dispersed in 4 mL hexane again at 3000 rpm for 5 min. The upper colloids were used to the characterization of optical properties and the ion exchange for PL, TCSPC, *etc*. We applied 2mL colloidal NCs evenly drip onto 4 cm^2 FTO and dried it at 25 °C for making the film to test the stability (Water and thermal stabilities). In addition, the precipitate was dried to test as XRD, *etc*.

Anion exchange:

According to our previous works.[1-3] Typically, 10 μL of ethanol solution of LiI or LiCl reagents were added to 1 mL of as-prepared NCs. The entire exchange reaction was completed in 10 s, and the colloids (for PL) were separated at 8000 rpm for 4 min to obtain powders (for XRD), which were dispersed in 4 mL toluene again at 3000 rpm for 4 min to PL characterization.

Characterization

TEM was measured by Netherlands Talos F200s microscope with high-resolution TEM images (FEI Tecnai G20). X-ray diffraction (XRD, Bruker D8 Advance) were obtained by X-ray diffraction under Cu Kαradiation at 45 kV and 40 mA at room temperature. Pb/M (M=Ni^{2+}, Cu^{2+} and Zn^{2+} reagents) doping molar ratios were analyzed by EDX in SEM. The PLQY was measured by C9920-02 (Hamamatsu photonics K.K., Japan). UV-vis absorption was obtained by Shimadzu UV-2550, China. XPS spectra were obtained using a Thermo-Fisher ESCA-LAB 250Xi. The steady state PL spectra and the TCSPC were tested by Florolog-3 (Horiba, USA).

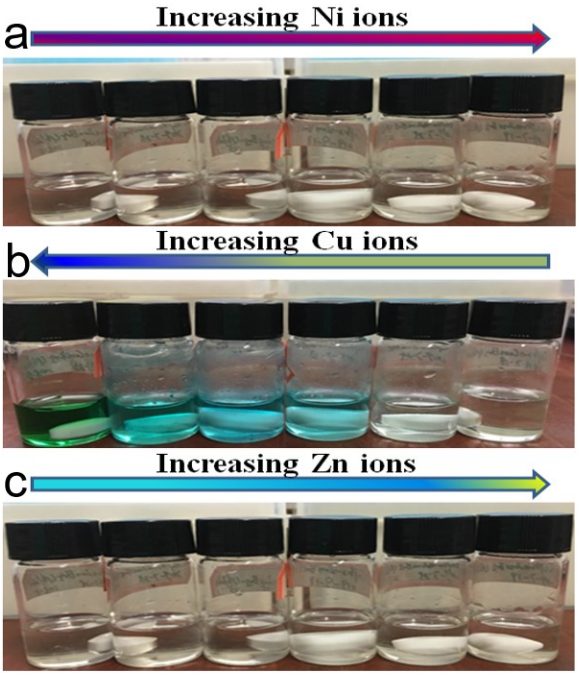

Fig. S1 The perovskite precursor solution with increasing concentration of transition metals: (a) Ni^{2+}-doped, (b) Cu^{2+}-doped, and (c) Zn^{2+}-doped perovskite precursor solution.

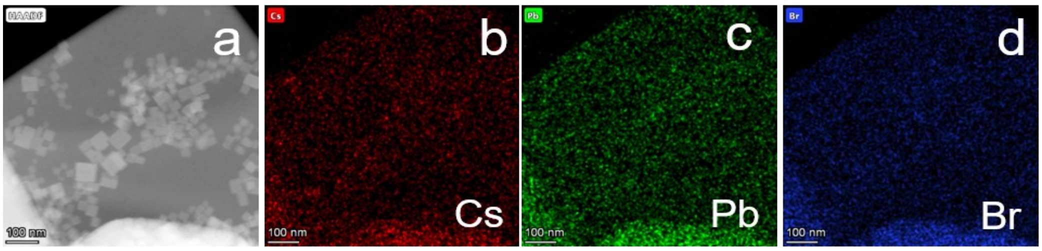

Fig. S2 (a) TEM image of undoped $CsPb_2Br_5/CsPbBr_3$ NCs. (b)-(d) Elemental distribution mapping images of the Cs, Pb and Br in film detected by EDS mapping, respectively.

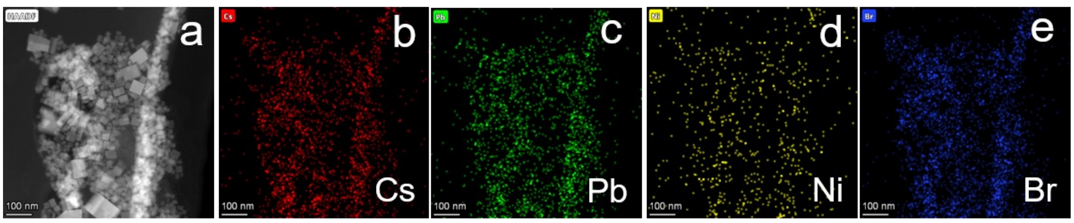

Fig. S3 (a) TEM image of Ni^{2+}-doped $CsPb_2Br_5/CsPbBr_3$ NCs. (b)-(e) Elemental distribution mapping images of the Cs, Pb, Ni and Br in film detected by EDS mapping, respectively.

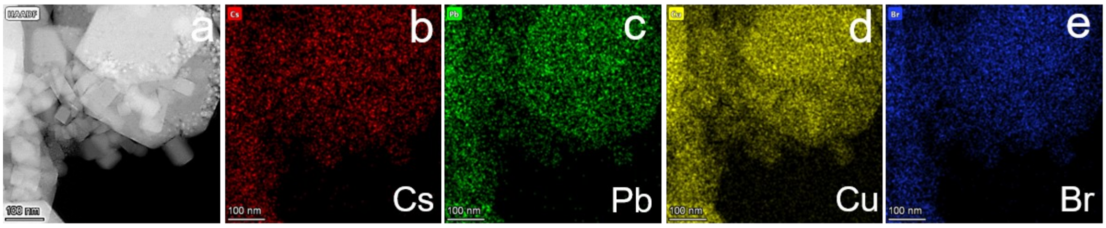

Fig. S4 (a) TEM image of Cu^{2+}-doped $CsPb_2Br_5/CsPbBr_3$ NCs. (b)-(e) Elemental distribution mapping images of the Cs, Pb, Cu and Br in film detected by EDS mapping, respectively.

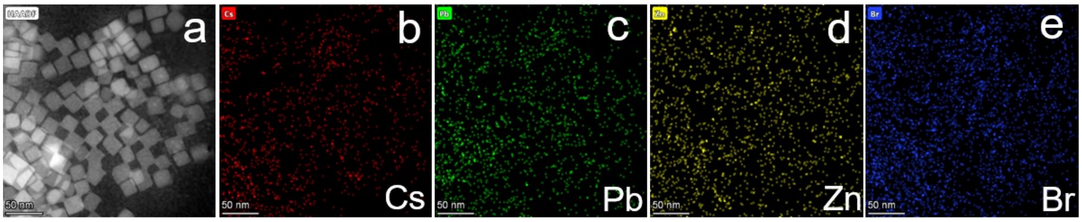

Fig. S5 (a) TEM image of Zn^{2+}-doped $CsPb_2Br_5/CsPbBr_3$ NCs. (b)-(e) Elemental distribution mapping images of the Cs, Pb, Zn and Br in film detected by EDS mapping, respectively.

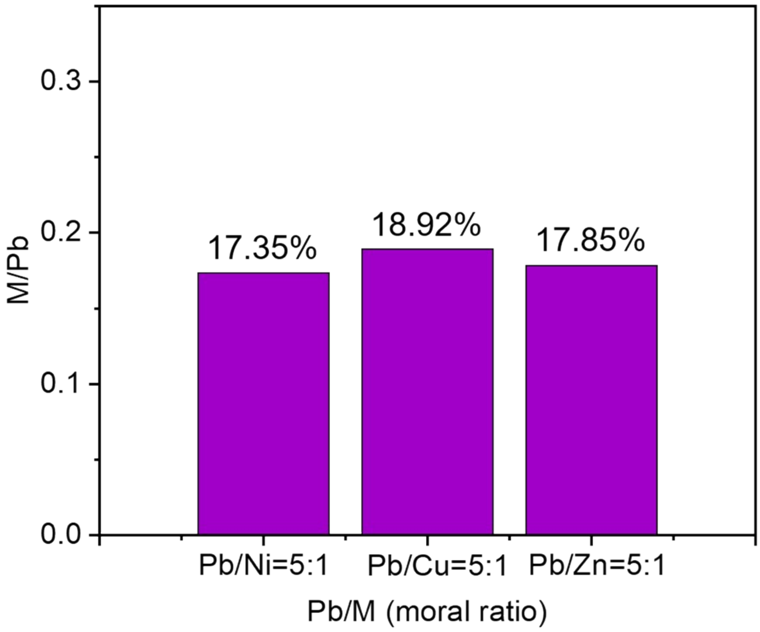

Fig. S6 The M/Pb values for the transition metal(II)-doped $CsPb_2Br_5/CsPbBr_3$ NCs (determined via SEM-EDX) as a function of the different molar feed ratio of $PbBr_2$ and MBr_2 used in the synthesis (M=$Ni^{2+}/Cu^{2+}/Zn^{2+}$, respectively).

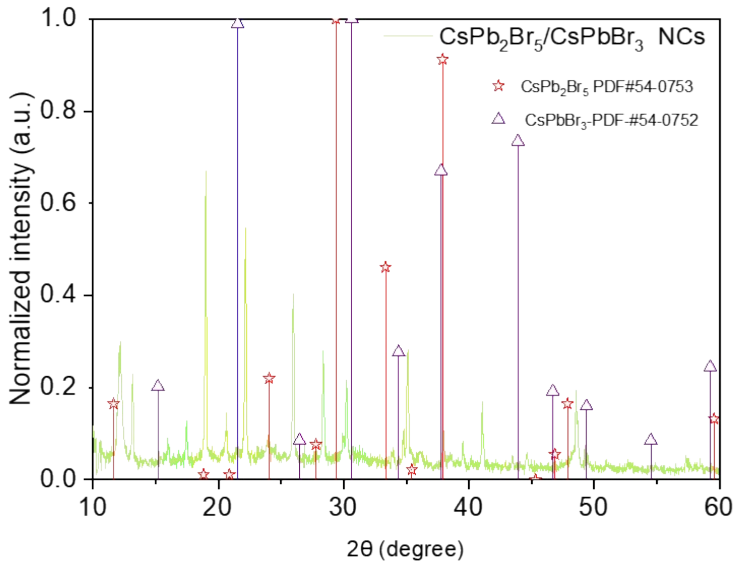

Fig. S7 The XRD pattern of as-obtained $CsPb_2Br_5/CsPbBr_3$ NCs, together with the standard pattern of $CsPb_2Br_5$ (red pentacle) and $CsPbBr_3$ (blue triangle).

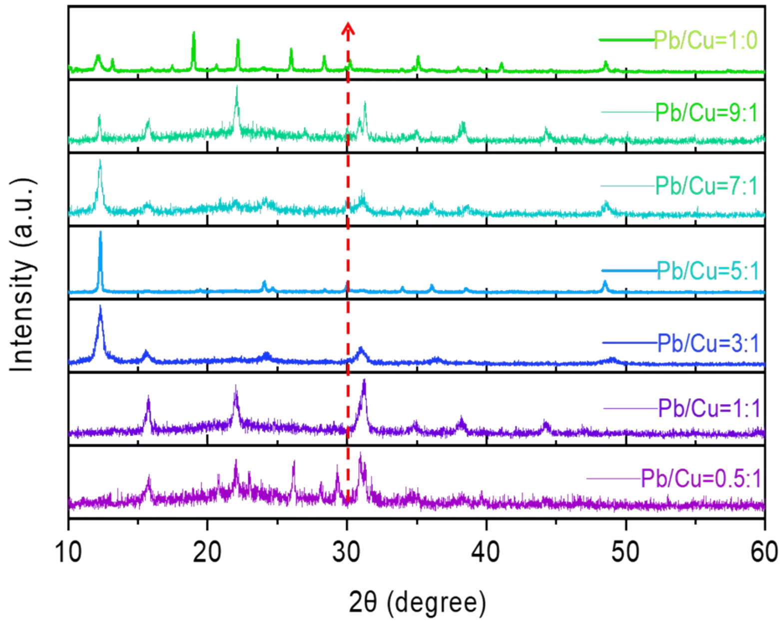

Fig. S8 The XRD patterns of the Cu^{2+}-doped $CsPb_2Br_5/CsPbBr_3$ NCs.

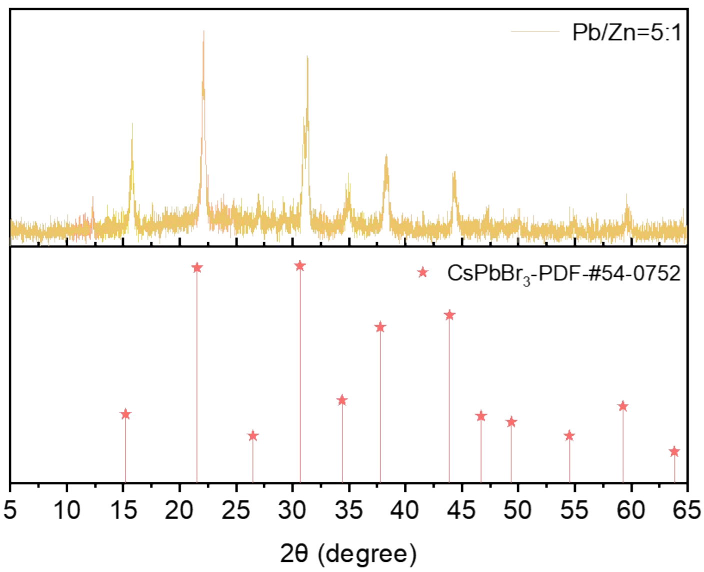

Fig. S9 The XRD pattern of Zn^{2+}-doped $CsPb_2Br_5/CsPbBr_3$ NCs, together with the standard pattern of $CsPbBr_3$ (red pentacle).

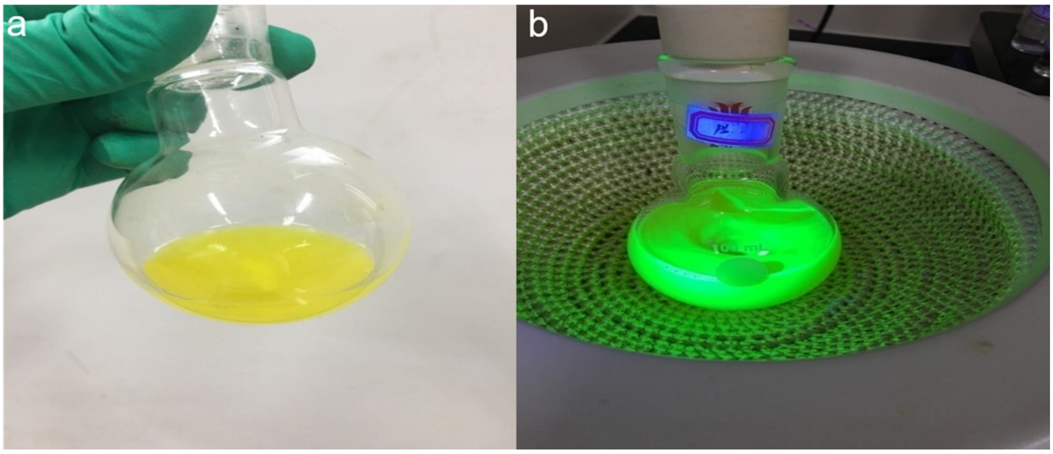

Fig. S10 The photos of colloidal $CsPb_2Br_5/CsPbBr_3$ NCs solution under ambient conditions (a), and under 365 nm light irradiation (b).

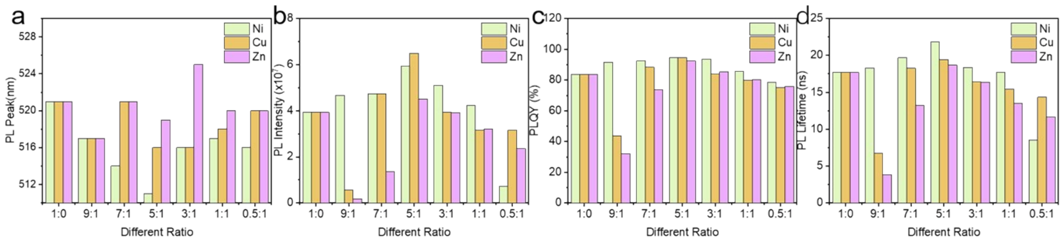

Fig. S11 Statistical plots of optical properties (PL peak and intensity, PLQY and PL lifetime) of different NCs.

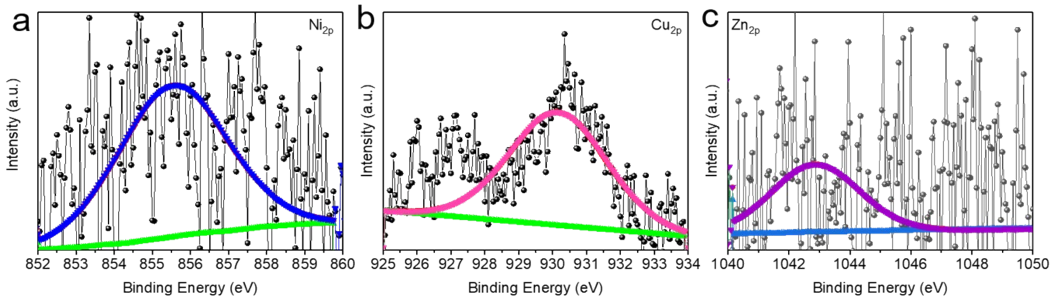

Fig. S12 The high-resolution XPS spectra measurement in the binding energy of Ni_{2p}, Cu_{2p}, and Zn_{2p}.

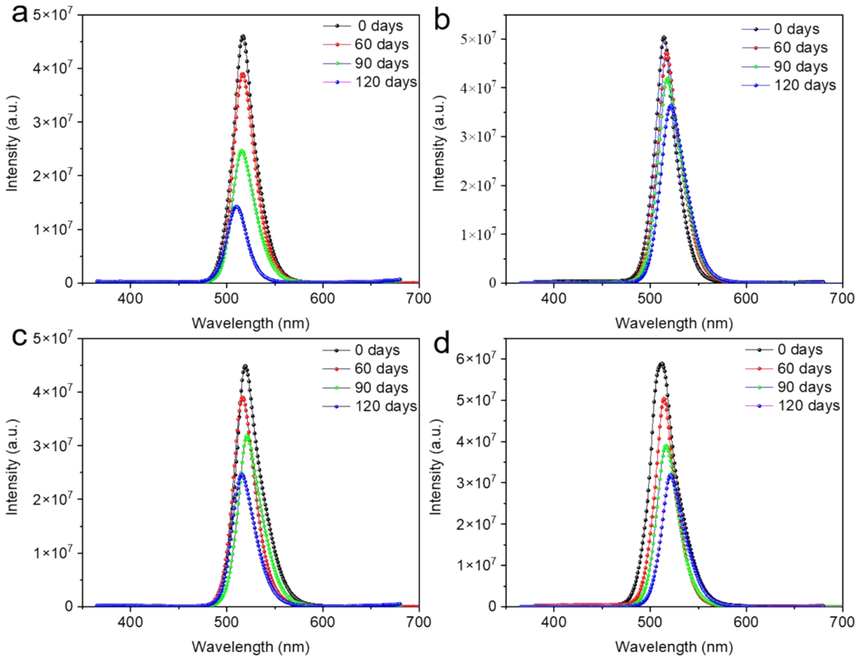

Fig. S13 PL spectrum of doped $CsPb_2Br_5/CsPbBr_3$ NCs in solution: (a) undoped $CsPb_2Br_5/CsPbBr_3$ NCs. (b) Ni^{2+}-doped $CsPb_2Br_5/CsPbBr_3$ NCs (Pb/Ni=5:1), (c) Cu^{2+}-doped $CsPb_2Br_5/CsPbBr_3$ NCs (Pb/Cu=5:1) and (d) Zn^{2+}-doped $CsPb_2Br_5/CsPbBr_3$ NCs (Pb/Zn=5:1), respectively.

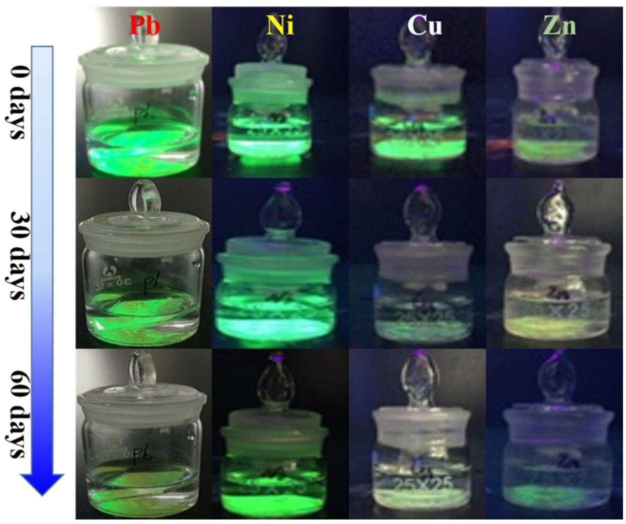

Fig. S14 The images of the films of based on the transition metal(II)-doped $CsPb_2Br_5/CsPbBr_3$ NCs under the 4 mL water at 30 ^oC.

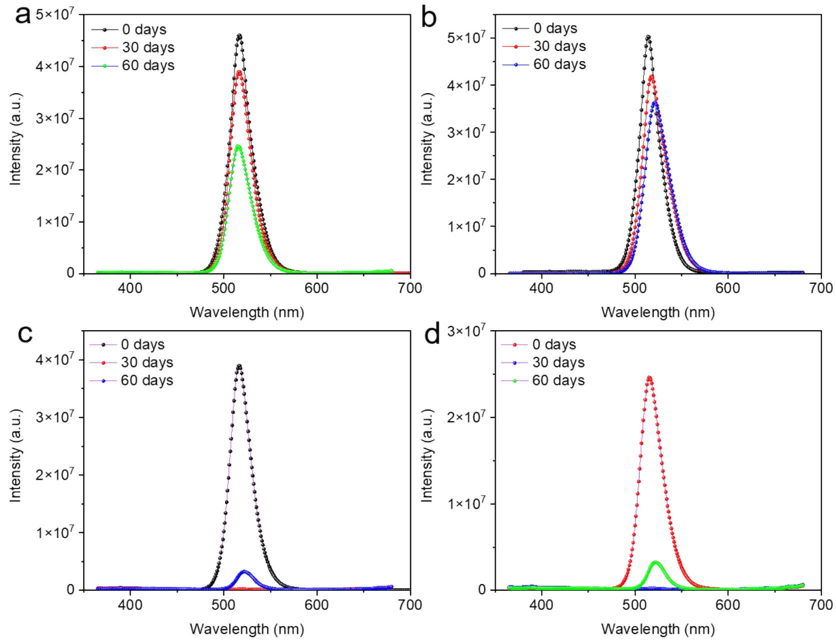

Fig. S15 PL spectrum of the films of based NCs under the 4 mL water: (a) undoped $CsPb_2Br_5/CsPbBr_3$ NCs. (b) Ni^{2+}-doped $CsPb_2Br_5/CsPbBr_3$ NCs (Pb/Ni=5:1), (c) Cu^{2+}-doped $CsPb_2Br_5/CsPbBr_3$ NCs (Pb/Cu=5:1) and (d) Zn^{2+}-doped $CsPb_2Br_5/CsPbBr_3$ NCs (Pb/Zn=5:1), respectively.

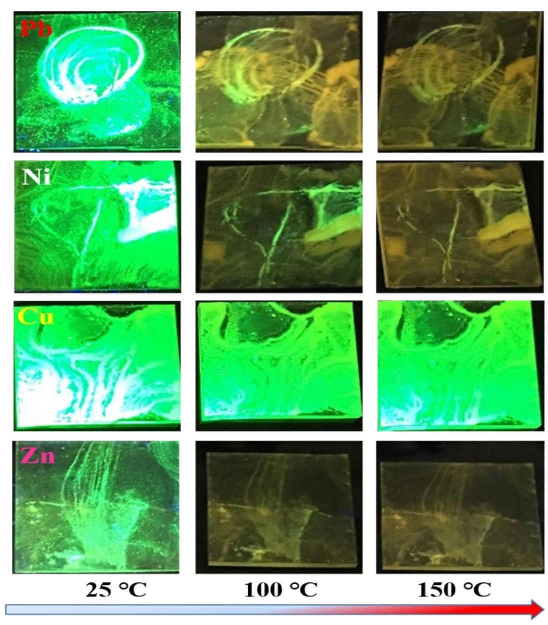

Fig. S16 The photos of the films of based on the transition metal(II)-doped $CsPb_2Br_5/CsPbBr_3$ NCs with the different temperature.

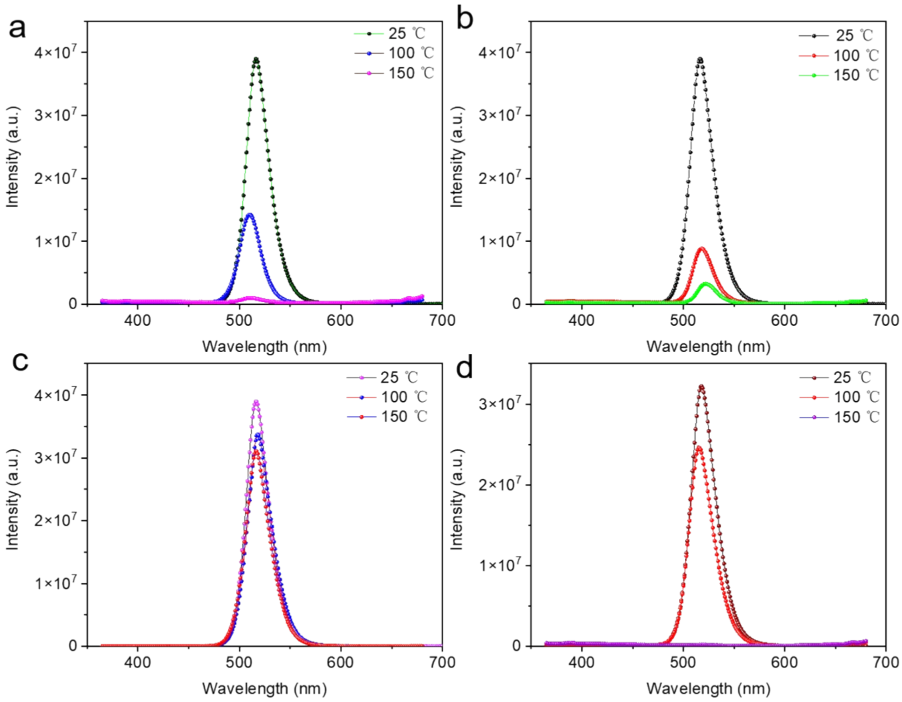

Fig. S17 Temperature-dependent PL spectrum of the films of based NCs: (a) Pure $CsPb_2Br_5/CsPbBr_3$ NCs. (b) Ni^{2+}-doped $CsPb_2Br_5/CsPbBr_3$ NCs (Pb/Ni=5:1), (c) Cu^{2+}-doped $CsPb_2Br_5/CsPbBr_3$ NCs (Pb/Cu=5:1) and (d) Zn^{2+}-doped $CsPb_2Br_5/CsPbBr_3$ NCs (Pb/Zn=5:1), respectively.

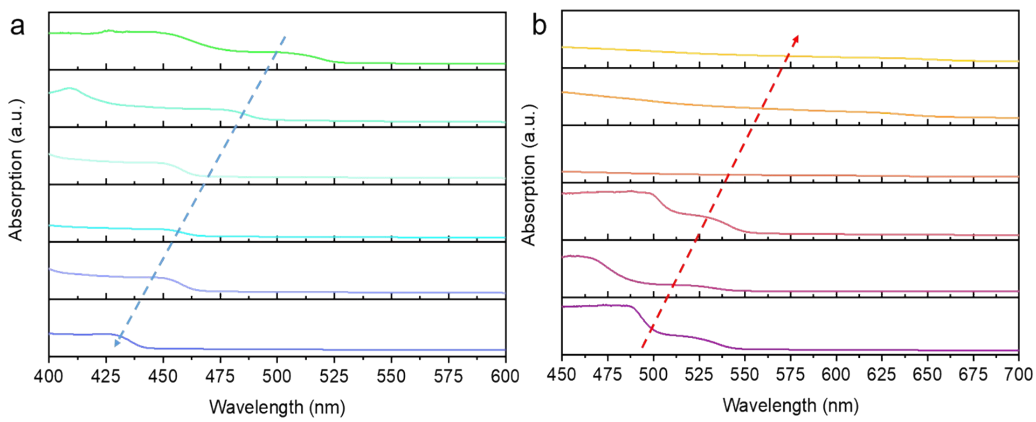

Fig. S18 Evolution of the optical absorption spectra of doped $CsPb_2Br_5/CsPbBr_3$ NCs with increasing quantities of anion-exchange of (a) Cl^-, and I^- (b), respectively.

Table S1. Fitted PL lifetime of Ni^{2+}-doped $CsPb_2Br_5/CsPbBr_3$ NCs (by bi-exponential decay).

Ni^{2+}-doped $CsPb_2Br_5/CsPbBr_3$ NCs (Pb/Ni)	Em-Wavelength (nm)	Intensity ($x10^7$ a. u.)	FWHM (nm)	T_{ave} (ns)	PLQY (%)	Γ_{rad} μs^{-1}	$\Gamma_{non\text{-}rad}$ μs^{-1}
1:0	521	3.933	23	17.69	83.7	47.31	9.21
9:1	517	4.673	29	18.30	91.5	49.99	4.64
7:1	514	4.739	24	19.67	92.4	46.96	3.86
5:1	511	5.943	28	21.81	94.6	43.36	2.47
3:1	516	5.096	28	18.36	93.7	51.02	3.43
1:1	517	4.228	26	17.72	85.7	48.35	8.06
0.5:1	516	0.718	28	8.50	78.6	920.39	25.15

Notes: using the values of PLQY[4] and average lifetimes, we can evaluate the radiative and non-radiative decay rates of these QDs based on the following equations:[5]

$$\Gamma_{rad} = \frac{PLQY}{\tau_{ave}} \quad (1)$$

$$\Gamma_{non\text{-}rad} = \frac{1}{\tau_{ave}} - \Gamma_{rad} = \frac{1-PLQY}{\tau_{ave}} \quad (2)$$

Among them, Γ_{rad} stands for radiative recombination rates; $\Gamma_{non-rad}$ notes the non-radiative recombination rates; τ_{ave} notes the average lifetime.

Table S2. Fitted PL lifetime of Cu^{2+}-doped $CsPb_2Br_5/CsPbBr_3$ NCs (by bi-exponential decay).

Cu^{2+}-doped $CsPb_2Br_5/CsPbBr_3$ NCs (Pb/Cu)	Em-Wavelength (nm)	Intensity (10^7 a. u.)	FWHM (nm)	T_{ave} (ns)	PLQY (%)	Γ_{rad} μs^{-1}	$\Gamma_{non\text{-}rad}$ μs^{-1}
1:0	521	3.933	23	17.69	83.7	47.31	9.21
9:1	517	0.570	20	6.75	43.6	64.58	83.54
7:1	521	4.737	26	18.25	88.3	48.39	6.41
5:1	516	6.492	29	19.45	94.5	48.56	2.82
3:1	516	3.943	28	16.43	84.1	51.18	9.67
1:1	518	3.160	27	15.44	79.8	51.69	13.08
0.5:1	520	3.150	25	14.36	75.1	52.30	17.34

Table S3. Fitted PL lifetime of Zn^{2+}-doped $CsPb_2Br_5/CsPbBr_3$ NCs (by bi-exponential decay).

Zn^{2+}-doped $CsPb_2Br_5/CsPbBr_3$ NCs (Pb/Zn)	Em-Wavelength (nm)	Intensity (10^7 a. u.)	FWHM (nm)	T_{ave} (ns)	PLQY (%)	Γ_{rad} μs^{-1}	$\Gamma_{non\text{-}rad}$ μs^{-1}
1:0	521	3.933	23	17.69	83.7	47.31	9.21
9:1	517	0.168	23	3.84	32.1	83.59	176.82
7:1	521	1.356	25	13.19	73.6	55.80	20.01
5:1	519	4.514	28	18.69	92.5	49.48	4.01
3:1	525	3.920	28	16.38	85.3	52.07	8.97
1:1	520	3.204	28	13.53	80.4	59.43	14.48
0.5:1	520	2.357	28	11.67	75.8	64.93	20.73

Table S4. Optical parameters of the transition metal(II)-doped $CsPb_2Br_5/CsPbBr_3$ NCs exchange with Cl^-.

LiCl concentration	Em-Wavelength (nm)	Band energy[a] (eV)	FWHM (nm)
0.4578 M	452	2.75	16
0.2289M	465	2.67	17
0.1144M	487	2.55	21
0.0572M	500	2.49	23
0.0382M	509	2.44	20
0.0286M	515	2.41	22

[a]The acquired diffuse reflectance (DR) spectrum was converted to the Kubelka-Munk function F(R),[6] which is approximately proportional to the absorption coefficient, according to the relation F(R)=(1-R)/(2R), where R is the diffuse reflectivity.

Table S5. Optical parameters of the transition metal(II)-doped $CsPb_2Br_5/CsPbBr_3$ NCs exchange with I^-.

LiI concentration	Em-Wavelength (nm)	Band energy[a] (eV)	FWHM (nm)
0.0085M	527	2.36	22
0.0106M	553	2.25	30
0.0142M	587	2.12	28
0.0213M	626	1.99	38
0.0425M	640	1.94	37
0.0850M	654	1.90	37

References

1 J. Xun, J. Deng, W. Shen, M. Li and R. He, *Opt. Mater.*, 2021, **122**, 111799.

2 J. Xun, J. Deng, W. Shen, M. Li and R. He, *J. Alloys Compd.*, 2021, **872**, 159612.

3 J. Deng, J. Xun and R. He, *Opt. Mater.*, 2020, **99**, 109528.

4 Q. A. Akkerman, V. D'Innocenzo, S. Accornero, A. Scarpellini, A. Petrozza, M. Prato and L. Manna, *J. Am. Chem. Soc.*, 2015, **137**, 10276-10281.

5 E. Torres and T. P. Kaloni, *Comp. Mater. Sci.*, 2020, **171**, 109237.

6 Y. Yamada, T. Nakamura, M. Endo, A. Wakamiya and Y. Kanemitsu, *Appl. Phys. Express.*, 2014, **7**, 032302.